

Holes U1415D and U1415E¹

K.M. Gillis, J.E. Snow, A. Klaus, G. Guerin, N. Abe, N. Akizawa, G. Ceuleneer, M.J. Cheadle, Á. Adrião, K. Faak, T.J. Falloon, S.A. Friedman, M.M. Godard, Y. Harigane, A.J. Horst, T. Hoshide, B. Ildefonse, M.M. Jean, B.E. John, J.H. Koepke, S. Machi, J. Maeda, N.E. Marks, A.M. McCaig, R. Meyer, A. Morris, T. Nozaka, M. Python, A. Saha, and R.P. Wintsch²

Chapter contents

Operations.....	1
Igneous petrology.....	2
Metamorphic petrology.....	3
Structural geology.....	4
Inorganic geochemistry.....	5
Physical properties.....	5
References.....	5
Figures.....	7
Tables.....	15

Operations

The locations of Integrated Ocean Drilling Program Holes U1415D and U1415E (see Fig. F8 in the “Expedition 345 summary” chapter [Gillis et al., 2014b]) were selected to test sediment thickness and seafloor drilling conditions, with the aim of finding a suitable site for establishing a deep hole. Hole operations are summarized in Table T1 and outlined below. All times are ship local time (UTC – 7 h).

Near-bottom 3.5 kHz pinger and camera survey

Following the completion of operations in Hole U1415C and while still at that location, we assembled a new bottom-hole assembly (BHA) and lowered the bit to just above the seafloor. We lowered the camera system with the 3.5 kHz pinger attached and initiated a new survey of the seafloor and near-subbottom (see Table T1 and Fig. F3 in the “Bench site survey” chapter [Gillis et al., 2014a]). The 3.5 kHz pinger ceased transmitting ~100 m into the survey, and we shortened the survey, which was completed using only visual observations of the seafloor.

Hole U1415D drilling operations

A new location to drill was selected, and the ship moved into position for Hole U1415D. Following a routine slip and cut of the drill line, we observed the bit tag seafloor at 4850.8 meters below rig floor (mbrf). Hole U1415D was spudded at 2355 h on 24 December 2012. We conducted a jet-in test that advanced 4.2 m into the seafloor. The bit was pulled clear of the seafloor at 0026 h on 25 December, ending Hole U1415D.

Hole U1415E drilling operations

After the camera system was recovered, we installed a fresh core barrel and spudded Hole U1415E at 0330 h on 25 December 2012. This hole was rotary cored from seafloor (4850.8 mbrf) to 22.2 meters below seafloor (mbsf) (4873.0 mbrf). Cores 345-U1415E-1R and 2R were recovered (0–15.3 mbsf) with 5% recovery. Very difficult hole conditions were encountered throughout the interval, with high pump pressure, high drilling torque, and hole collapse occurring every time the bit was picked up off bottom. While cutting Core 3R (15.3–22.2 mbsf), the pump pressure dropped from 800 to 350 psi at 70 strokes/min, top drive torque dropped off sig-

¹Gillis, K.M., Snow, J.E., Klaus, A., Guerin, G., Abe, N., Akizawa, N., Ceuleneer, G., Cheadle, M.J., Adrião, Á., Faak, K., Falloon, T.J., Friedman, S.A., Godard, M.M., Harigane, Y., Horst, A.J., Hoshide, T., Ildefonse, B., Jean, M.M., John, B.E., Koepke, J.H., Machi, S., Maeda, J., Marks, N.E., McCaig, A.M., Meyer, R., Morris, A., Nozaka, T., Python, M., Saha, A., and Wintsch, R.P., 2014. Holes U1415D and U1415E. *In* Gillis, K.M., Snow, J.E., Klaus, A., and the Expedition 345 Scientists, *Proc. IODP, 345*: College Station, TX (Integrated Ocean Drilling Program).

doi:10.2204/iodp.proc.345.106.2014

²Expedition 345 Scientists' addresses.



nificantly, and the driller noticed a string weight loss of ~10,000 lb, indicating a likely BHA failure. The drill string was recovered, and the fourth drill collar pin (first collar above the outer core barrel stand) had broken off. Besides the inner core barrel assembly, three drill collars and the entire outer core barrel assembly were lost in the hole. In addition, two other drill collars were bent. Only the uppermost stand of drill collars was in working condition.

Igneous petrology

Coring in Hole U1415E recovered 16 different igneous lithologic intervals from a surficial “rubble” zone, which was defined as lithologic Unit I (Fig. F1). Below, we give a brief lithologic description for each rock type recovered in the different intervals based on macroscopic and, where available, microscopic observations. Two different lithologic domains were defined one thin section from Hole U1415E. Therefore, a table is provided listing the corresponding thin section, the number and nature of the individual domains, the characteristics of the contact between the domains, as well as a link for the corresponding image of the thin section with the domain boundaries marked (Table T2).

Gabbro

Gabbro defines five intervals (Intervals 6, 9, 10, 12, and 13) from Unit I. In general, the gabbros are medium grained with equigranular to subophitic textures. Modally, gabbro consists of plagioclase (35%–65%) and clinopyroxene (35%–65%), with trace amounts of oxide. Plagioclase is medium grained and subhedral to euhedral with a lath-shaped habit. Clinopyroxene is medium grained and anhedral with an interstitial habit.

Olivine-bearing gabbro

Olivine-bearing gabbro defines three intervals (Intervals 1, 7, and 15) from Unit I. In general, the olivine-bearing gabbro is a medium-grained, equigranular to subophitic granular rock. Modally, olivine-bearing gabbro consists of olivine (2%–3%), plagioclase (60%–72%), and clinopyroxene (25%–40%), with trace amounts of oxide and occasionally trace orthopyroxene. Olivine is fine grained and subhedral to euhedral with a subequant habit. Plagioclase is fine grained and subhedral to euhedral with a tabular habit. Zoning in plagioclase is scarce. Clinopyroxene is fine to medium grained and anhedral with an interstitial habit.

Olivine gabbro

Olivine gabbro defines two intervals (Intervals 14 and 16) in Unit I. In general, olivine gabbro is medium grained equigranular granular rock. Modally, olivine gabbro consists of olivine (15%–20%), plagioclase (50%–70%), and clinopyroxene (10%–35%), with trace amounts of oxide. Olivine is fine grained and euhedral to subhedral with a subequant habit. Plagioclase is medium grained and subhedral to euhedral with a tabular habit. Clinopyroxene is medium to coarse grained with an anhedral interstitial habit.

Gabbronorite

Gabbronorite defines two intervals (Intervals 3 and 5) in Unit I. In general, gabbronorite is medium grained and inequigranular with seriate to subophitic textures (Fig. F2). Modally, gabbronorite consists of plagioclase (35%–60%), clinopyroxene (18%–20%), and orthopyroxene (20%–35%), with trace ($\leq 2\%$) oxide. Plagioclase is medium grained and subhedral to euhedral with a tabular habit. Clinopyroxene is medium grained and anhedral with an irregular interstitial to poikilitic habit. Orthopyroxene is anhedral with an irregular poikilitic habit (Fig. F3).

One gabbronorite sample (345-U1415E-1R-1, 21–23 cm) shows a patchy appearance resulting from the presence of two lithologically different domains consisting of orthopyroxene-bearing gabbro and disseminated oxide gabbronorite (Fig. F4; lithologies of the two domains are based on thin section descriptions). This feature was not observed in any other gabbro in Hole U1415E. A characteristic feature is the presence of orthopyroxene, oxide minerals and probably primary amphibole (now nearly completely altered to secondary amphibole), and oxide inclusions in plagioclase of the disseminated oxide gabbronorite, implying that this lithology is rather evolved compared to most other gabbroic lithologies recovered at Site U1415.

Troctolite

Troctolite occurs as a highly altered single piece in Hole U1415E (Interval 4; Fig. F5). The troctolite is a medium-grained equigranular rock. Modally, the troctolite consists of olivine (40%), plagioclase (45%), and clinopyroxene (15%), with trace amounts of oxide. Olivine is anhedral and completely altered. Plagioclase is anhedral to subhedral with a tabular habit. Clinopyroxene occurs as subhedral to euhedral prismatic grains.

Orthopyroxene-bearing olivine gabbro

Orthopyroxene-bearing olivine gabbro defines one interval (Interval 2) in Unit I. The highly altered orthopyroxene-bearing olivine gabbro is a medium-grained equigranular subophitic rock. Modally, orthopyroxene-bearing olivine gabbro consists of olivine (5%–7%), plagioclase (50%), clinopyroxene (40%), and orthopyroxene (3%), with trace amounts of oxide. Olivine is fine grained and euhedral to subhedral with subequant habit. Plagioclase is medium grained and euhedral to subhedral with a tabular habit. Clinopyroxene is medium grained and anhedral with a subequant habit. Orthopyroxene is euhedral to subhedral with an equant habit.

Anorthositic gabbro

Anorthositic gabbro defines a single interval (Interval 8) in Unit I (Thin Section 4; Sample 345-U1415E-2R-1, 0–3 cm). The highly altered anorthositic gabbro is a medium-grained equigranular granular rock. Modally, anorthositic gabbro consists of plagioclase (90%) and clinopyroxene (10%). Plagioclase is medium grained and subhedral with a tabular habit. Clinopyroxene appears to be medium grained and anhedral with an interstitial habit.

Doleritic gabbro

Doleritic gabbro defines a single interval (Interval 11) in Unit I. Doleritic gabbro is a fine-grained equigranular ophitic rock. Modally, doleritic gabbro consists of plagioclase (50%) and clinopyroxene (50%), with trace amounts of oxide. Plagioclase is fine grained and euhedral to subhedral with a lath-like habit. Clinopyroxene is fine grained and anhedral with an interstitial to ophitic habit.

Metamorphic petrology

All of the recovered lithologies show some degree of hydration and exhibit metamorphism over greenschist to subgreenschist facies conditions; because the core is from a rubble unit, no patterns of alteration can be established.

Background alteration

Primary mineral replacement ranges from 10% to 60%. Most of the secondary minerals are visible to the naked eye. In the recovered gabbroic rock, pyroxene was moderately to strongly altered to pale green amphibole, and olivine in these samples was strongly (60% to >90%) replaced by serpentine with mesh textures. Troctolite (Sample 345-U1415E-1R-1, 29.5–39.5 cm [Piece 4]) recovered from this hole was

strongly (60% to >90%) altered, showing tremolite-chlorite corona textures between olivine and plagioclase, later serpentinization and replacement of plagioclase by prehnite and hydrogarnet, and finally late replacement of olivine by talc. Incipient corona textures (concentric zones of chlorite replacing plagioclase and tremolite ± talc ± chlorite replacing olivine) are present. The olivine corona textures appear to result in a volume increase during the serpentinization of olivine. Anorthositic gabbro (Sample 345-U1415E-2R-1, 0–6 cm [Piece 1]) was extensively replaced by prehnite, clinozoisite, and chlorite associated with a vein of similar mineralogy. In most of the lithologies recovered in Hole U1415E, plagioclase is slightly altered to secondary plagioclase, prehnite, and chlorite. Plagioclase is commonly altered to chlorite along grain boundaries with relict olivine. Some of the rock shows evidence for cataclasis, and adjacent to these zones plagioclase is highly fractured with minor replacement by secondary plagioclase and prehnite along the fracture surfaces.

In one orthopyroxene-bearing gabbro sample (345-U1415E-1R-1, 21–23 cm [Piece 3]; Table T2), alteration was minimal, although a fine-grained patch appeared to be developing grain boundary migration within the ophitic texture. In this case, the ophitic texture is still visible but the grain boundaries are strongly sutured (Fig. F6). This texture may represent incipient granoblastic recrystallization.

Veins

Veins are mostly thin (1–2 mm wide) and isolated and are dominated by subgreenschist facies minerals including clay minerals, actinolite, and prehnite. In olivine-rich lithologies, serpentine veins are also present. Microscopic zeolite veins often crosscut plagioclase crystals. Vein shapes are irregular and are characterized by sharp contacts with the host rock, but several parallel veins of identical nature may be present in one single piece. Most of the pieces recovered in Hole U1415E contain one or two veins (see “[Structural geology](#)”). A small amount of material collected in Sample 345-U1415E-2R-1, 6–9 cm (Piece 2) is identified as gabbro but may in fact be fragments of material sampling a larger vein. The composition of this material includes abundant prehnite, chlorite, and secondary plagioclase.

Rock coatings

The uppermost two pieces of olivine-bearing gabbro (0–0.2 mbsf) have a thin manganese-bearing phyllosilicate (ganophyllite) surface coating confirmed by X-ray diffraction, suggesting possible seafloor weathering.

Metamorphic conditions and degrees of alteration

The alteration observed in these samples is variable, as would be expected in rocks from a rubble unit. The dominant alteration of all of the rock recovered is subgreenschist to possibly lower amphibolite facies. The alteration predominantly affects pyroxene and olivine; primary plagioclase is largely unaltered, except where it is in contact with relict olivine or where fractured in cataclastic zones. The presence of zeolite veins indicates that some of the hydration occurred at or below zeolite facies conditions.

Structural geology

All core pieces from Hole U1415E are relatively small (11 cm maximum length), were not cored or oriented, and comprise surficial rubble (lithologic Unit I).

Magmatic structures

The earliest history of rock in Hole U1415E is constrained by magmatic fabrics preserved in the recovered gabbroic rock. No magmatic layering was observed, possibly because of the small size of recovered pieces. Three medium- and fine-grained gabbro pieces exhibit planar, weak- to moderate-strength foliation defined by the shape-preferred orientation (SPO) of plagioclase (Sample 345-U1415E-1R-1 [Pieces 1, 5, and 6]). The plagioclase crystals are 1–2 mm long with shape anisotropy commonly 5:1 and ranging up to 10:1 in some crystals. One medium-grained olivine gabbro exhibits weak plagioclase and olivine SPO (Sample 1R-1 [Piece 2]). All other pieces show either no magmatic foliation or were too small to enable recognition of foliation. Consequently, >52% of the core has magmatic foliation.

Thin section observations show that the magmatic foliation is defined by both the preferred orientation and shape anisotropy of 1–2 mm long plagioclase crystals. The plagioclase crystals are often tabular with albite twin planes parallel to the long axes of the crystals. Microscopic observations show that plagioclase crystals in one fine-grained gabbro (Sample 1R-1, 41–43 cm [Piece 5]) are commonly elongate and exhibit weak plagioclase SPO. The crystals show only limited annealing but noticeable deformation twinning, undulose extinction, and bending (Fig. F7A, F7B), with the apparent fold hinges lying within the plane of the foliation. Occasionally, bending led to subgrain development. Minor undulose extinction, subgrain formation, and kink bands are also noted in several clinopyroxene grains. Another

fine-grained gabbro (Sample 1R-1, 21–23 cm [Piece 3]) exhibits very weak foliation defined by plagioclase SPO (Fig. F7C). Plagioclase crystals in Piece 3 show rare submagmatic deformation twins and/or bent grains. In part of the thin section, seriate plagioclase grain boundaries are common, suggesting grain boundary migration that may result during subsolidus recrystallization.

The random distribution of plagioclase grains showing deformation twins in the core, the common orientation of fold hinges associated with bent grains, and the fact that some plagioclase grains appear bent around undeformed clinopyroxene crystals are suggestive that these crystal-plastic fabrics formed under hypersolidus conditions with some melt present.

Crystal-plastic deformation

No structurally continuous subsolidus crystal-plastic deformation was observed in the recovered sections.

Cataclastic deformation

Macroscopically, virtually all recovered pieces from Cores 345-U1415E-1R and 2R show limited brittle deformation restricted to several pieces hosting open fractures. These open fractures have no apparent offset and low density (<1 or 1–5 fractures per 10 cm). Section 345-U1415E-1R-1 (Piece 1) appears to be a shear phacoid with angular faces showing weakly developed slickensides.

Alteration veins

Alteration veins are present in 9 of the 14 pieces recovered in Cores 345-U1415E-1R and 2R (~65% of the pieces). When present, vein density is always low, with less than a few veins per 10 cm of recovery, and all veins are very thin (maximum thickness is <0.1 cm, in most cases <0.05 cm). Accordingly, alteration veins represent <<1% of the core volume. Where present, vein length generally exceeds the width of the core (6 cm), although vein terminations (vein tips) are frequently observed. Contacts with the gabbroic host are generally clear (Fig. F8), with only rare alteration halos observed.

The geometry of alteration veins varies from rather irregular in shape to frequently curved and commonly forms networks of crosscutting veins with no marked preferred orientation. As most pieces are not oriented and the hole is interpreted to have drilled in talus, no orientation data were collected.

In thin section, varying combinations of actinolite, chlorite, serpentine, zoisite, prehnite, zeolite, serpentine, and clay are observed as vein-filling material and as a “secondary” assemblage showing pervasive replacement of primary igneous minerals (see “Met-

amorphous petrology). The same alteration mineralogy is also seen in veins with clear-cut boundaries, in veins with diffuse boundaries (alteration halos), and defining any pervasive alteration within the rock. Alteration veins cut primary igneous minerals that are, as a rule, much larger than the width of individual veins. Use of the term alteration veins implies formation of undeformed mineral veins, postdating any shearing. In contrast, sheared veins are described as cataclastic features. Veins (undeformed) are more common than the cataclastic features. In some veins, alteration minerals have a rather isotropic shape (mosaic textures), whereas in other veins alteration minerals (usually prehnite) are fibrous, with fiber orientation typically perpendicular to the vein walls.

Temporal evolution

Temporal evolution of structures recovered in Hole U1415E is, from oldest to youngest,

- Intrusion of fine- and medium-grained gabbroic and troctolitic rocks (Units 1–7),
- Magmatic fabric development (foliation),
- Limited crystal-plastic deformation in the mush and annealing of plagioclase,
- Vein formation, and
- Open fractures associated with late brittle faulting.

Details specific to structural features are illustrated with comments in STRUCTUR in **“Supplementary material.”**

Inorganic geochemistry

One gabbroic sample was selected in Hole U1415E (Sample 345-U1415E-1R-1, 44–47 cm) for geochemical analysis. Sample selection was based on discussion among representatives from all expertise groups within the shipboard scientific party. Inductively coupled plasma–atomic emission spectroscopy (ICP-AES) was used to determine major and trace element concentrations, and gas chromatography was used for S, H₂O, and CO₂ quantifications. Results are reported in Table T1 in the “Geochemistry summary” chapter (Gillis et al., 2014c). Major and trace elements are reported on a volatile-free basis.

Sample 345-U1415E-1R-1, 44–47 cm, is characterized by low volatile contents, with a 0.44 wt% loss on ignition, 0.95 wt% H₂O, and 0.09 wt% CO₂. These values are consistent with the moderate degree of alteration of the analyzed sample (~10%; see **“Metamorphic petrology”** and Hole U1415E thin section descriptions in **“Core descriptions”**). The sample has an Mg# (cationic Mg/[Mg + Fe]; all Fe as Fe²⁺) of 73; relatively high SiO₂ (51 wt%), Fe₂O₃^(T) (7.7

wt%), and TiO₂ (0.5 wt%) content; and low Cr (123 ppm) and Ni (67 ppm) concentrations, overlapping in composition with gabbroic rocks previously sampled at ODP Site 894 and along the Northern Escarpment of the Hess Deep Rift. This gabbroic rock plots at the most primitive end of the field of the Hess Deep gabbro and gabbroic rocks (Gillis, Mével, Allan, et al., 1993; Pedersen, et al., 1996; Natland and Dick, 1996; Hanna, 2004; Kirchner and Gillis, 2012).

Physical properties

The only measured physical properties of cores recovered in Hole U1415E are magnetic susceptibility and color reflectance. These data were acquired using the Section Half Multisensor Logger with a measurement interval of 2 cm. Raw data were uploaded to the Laboratory Information Management System database and subsequently filtered to remove spurious points that correspond to empty intervals in the liner, broken pieces, and pieces that were too small. Filtered data are available in PHYSPROP in **“Supplementary material.”** Magnetic susceptibility ranges from $\sim 200 \times 10^{-5}$ to 4500×10^{-5} SI. Color reflectance parameters L*, a*, and b* mean values are 32.7 ± 4.9 , -0.48 ± 0.74 , and -0.53 ± 1.19 , respectively.

References

- Gillis, K., Mével, C., Allan, J., et al., 1993. *Proc. ODP, Init. Repts.*, 147: College Station, TX (Ocean Drilling Program). doi:10.2973/odp.proc.ir.147.1993
- Gillis, K.M., Snow, J.E., Klaus, A., Guerin, G., Abe, N., Akizawa, N., Ceuleneer, G., Cheadle, M.J., Adrião, Á., Faak, K., Falloon, T.J., Friedman, S.A., Godard, M.M., Harigane, Y., Horst, A.J., Hoshide, T., Ildefonse, B., Jean, M.M., John, B.E., Koepke, J.H., Machi, S., Maeda, J., Marks, N.E., McCaig, A.M., Meyer, R., Morris, A., Nozaka, T., Python, M., Saha, A., and Wintsch, R.P., 2014a. Bench site survey. In Gillis, K.M., Snow, J.E., Klaus, A., and the Expedition 345 Scientists, *Proc. IODP, 345*: College Station, TX (Integrated Ocean Drilling Program). doi:10.2204/iodp.proc.345.103.2014
- Gillis, K.M., Snow, J.E., Klaus, A., Guerin, G., Abe, N., Akizawa, N., Ceuleneer, G., Cheadle, M.J., Adrião, Á., Faak, K., Falloon, T.J., Friedman, S.A., Godard, M.M., Harigane, Y., Horst, A.J., Hoshide, T., Ildefonse, B., Jean, M.M., John, B.E., Koepke, J.H., Machi, S., Maeda, J., Marks, N.E., McCaig, A.M., Meyer, R., Morris, A., Nozaka, T., Python, M., Saha, A., and Wintsch, R.P., 2014b. Expedition 345 summary. In Gillis, K.M., Snow, J.E., Klaus, A., and the Expedition 345 Scientists, *Proc. IODP, 345*: College Station, TX (Integrated Ocean Drilling Program). doi:10.2204/iodp.proc.345.101.2014
- Gillis, K.M., Snow, J.E., Klaus, A., Guerin, G., Abe, N., Akizawa, N., Ceuleneer, G., Cheadle, M.J., Adrião, Á., Faak, K., Falloon, T.J., Friedman, S.A., Godard, M.M.,

- Harigane, Y., Horst, A.J., Hoshide, T., Ildefonse, B., Jean, M.M., John, B.E., Koepke, J.H., Machi, S., Maeda, J., Marks, N.E., McCaig, A.M., Meyer, R., Morris, A., Nozaka, T., Python, M., Saha, A., and Wintsch, R.P., 2014c. Geochemistry summary. In Gillis, K.M., Snow, J.E., Klaus, A., and the Expedition 345 Scientists, *Proc. IODP*, 345: College Station, TX (Integrated Ocean Drilling Program). doi:10.2204/iodp.proc.345.114.2014
- Hanna, H.D., 2004. Geochemical variations in basaltic glasses from an incipient rift and upper level gabbros from Hess Deep, eastern equatorial Pacific [M.Sc. thesis]. Duke Univ., Durham.
- Kirchner, T.M., and Gillis, K.M., 2012. Mineralogical and strontium isotopic record of hydrothermal processes in the lower ocean crust at and near the East Pacific Rise. *Contrib. Mineral. Petrol.*, 164(1):123–141 doi:10.1007/s00410-012-0729-5
- Natland, J.H., and Dick, H.J.B., 1996. Melt migration through high-level gabbroic cumulates of the East Pacific Rise at Hess Deep: the origin of magma lenses and the deep crustal structure of fast-spreading ridges. In Mével, C., Gillis, K.M., Allan, J.F., and Meyer, P.S. (Eds.), *Proc. ODP, Sci. Results*, 147: College Station, TX (Ocean Drilling Program), 21–58. doi:10.2973/odp.proc.sr.147.002.1996
- Pedersen, R.B., Malpas, J., and Falloon, T., 1996. Petrology and geochemistry of gabbroic and related rocks from Site 894, Hess Deep. In Mével, C., Gillis, K.M., Allan, J.F., and Meyer, P.S. (Eds.), *Proc. ODP, Sci. Results*, 147: College Station, TX (Ocean Drilling Program), 3–19. doi:10.2973/odp.proc.sr.147.001.1996

Publication: 12 February 2014
MS 345-106

Figure F1. Rock types recovered from lithologic Unit I in Hole U1415E based on the macroscopic description of individual pieces (excluding two samples from ghost cores, Intervals G1 and G2). For clarity, only the principal rock names without any modifier are shown.

Hole U1415E

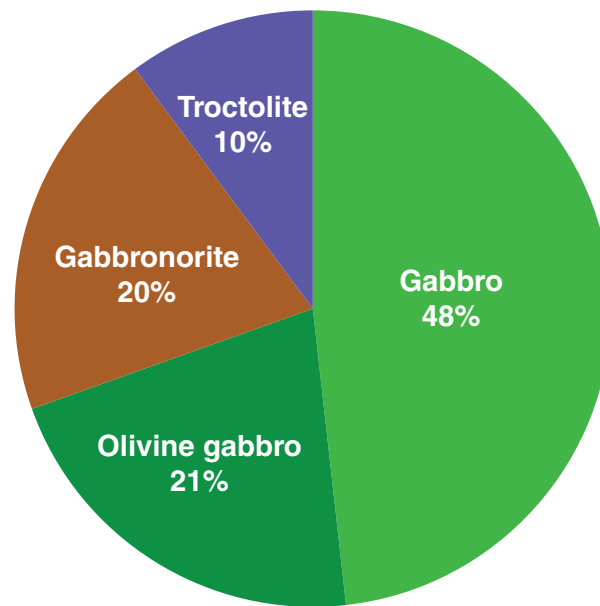


Figure F2. Gabbronorite (Thin Section 3; Sample 345-U1415E-1R-1, 41–43 cm [Piece 5]). Note the large, centimeter-sized prismatic orthopyroxene in the lower right part of the image. **A.** Plane-polarized light. **B.** Under crossed polars.

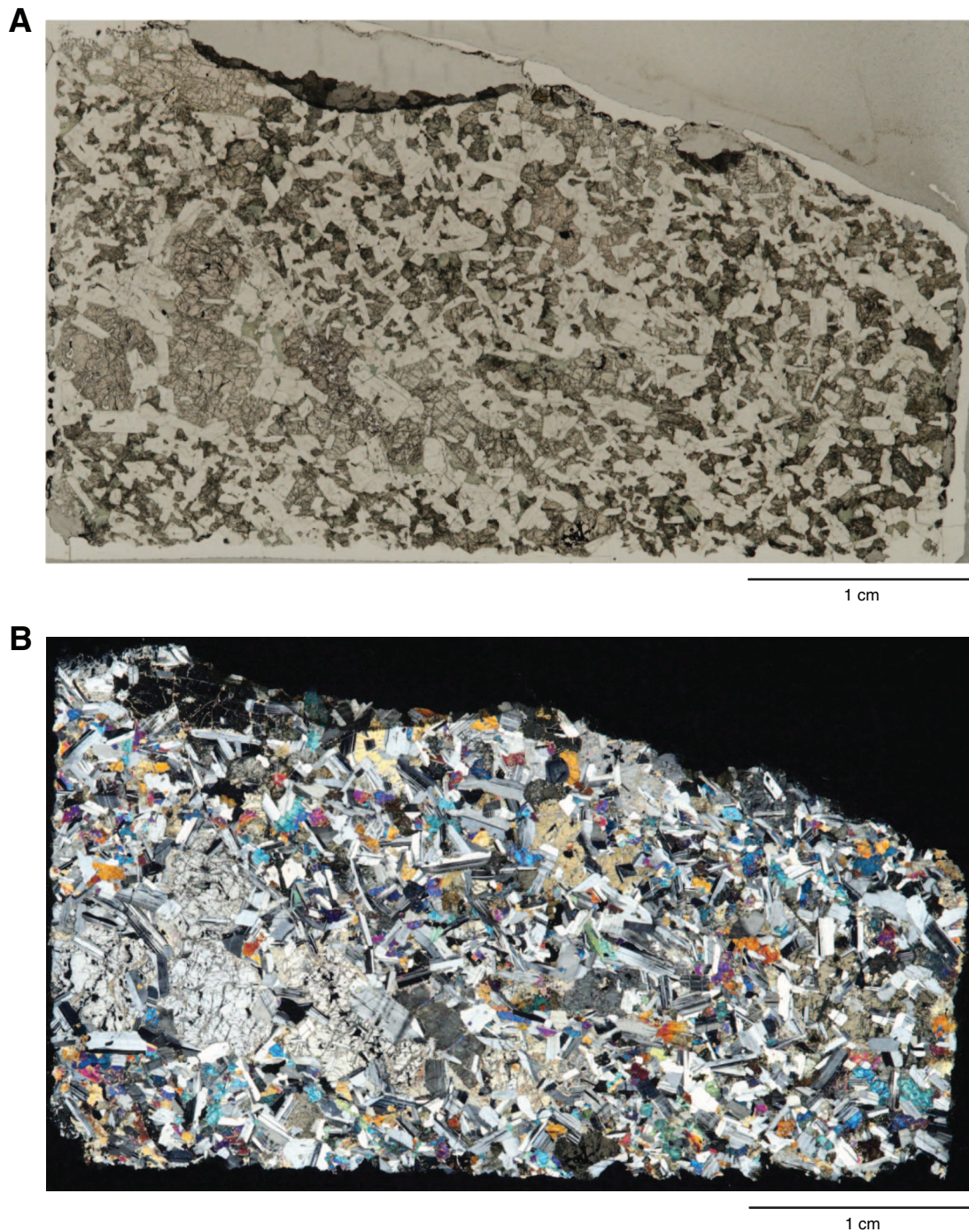


Figure F3. Typical occurrence of clinopyroxene (Cpx) and orthopyroxene (Opx) in gabbronorite (Thin Section 3; Sample 345-U1415E-1R-1, 41–43 cm [Piece 5]). Both minerals form anhedral crystals in the interstices of the plagioclase framework. Orthopyroxene is generally larger than clinopyroxene and tends to form a poikilitic texture. A. Plane-polarized light. B. Under crossed polars.

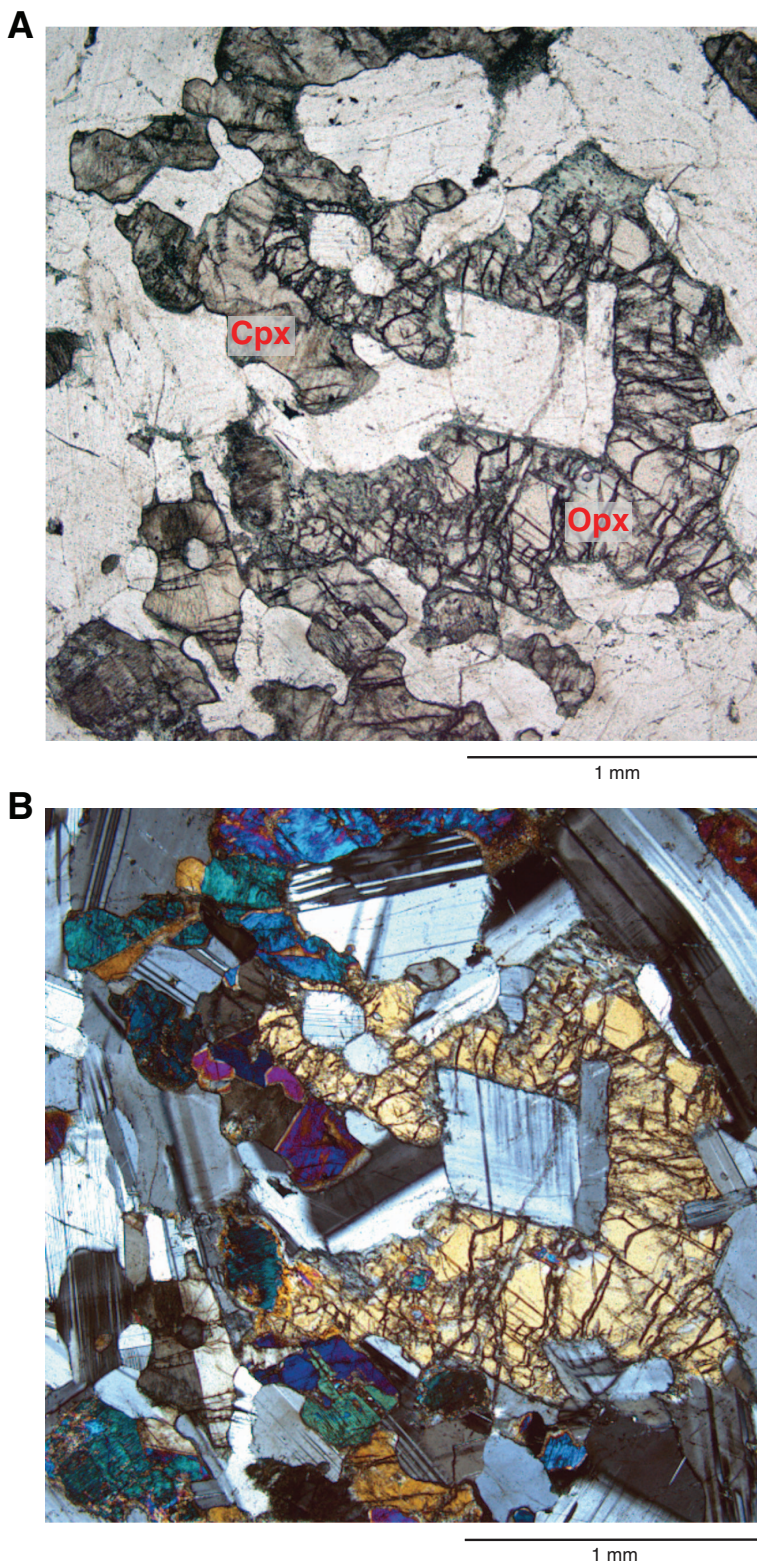


Figure F4. Orthopyroxene-bearing gabbro with two domains corresponding to different lithologies (Thin Section 1; Sample 345-U1415E-1R-1, 21–23 cm [Piece 3]; thin section length = 3.4 cm). **A, B.** Two domains (red lines) consisting of orthopyroxene-bearing gabbro and disseminated oxide gabbronorite: (A) under crossed polars; (B) plane-polarized light. Note the presence of large orthopyroxene (opx) and oxide minerals (black) in the disseminated oxide gabbronorite domain, whereas the orthopyroxene-bearing gabbro is characterized by clinopyroxene tending to form a subophitic network with more lath shaped plagioclase of smaller grain size. **C, D.** Plagioclase in disseminated oxide gabbronorite (yellow arrow) bears inclusions of oxide minerals; C is under crossed polars and D is under plane-polarized light.

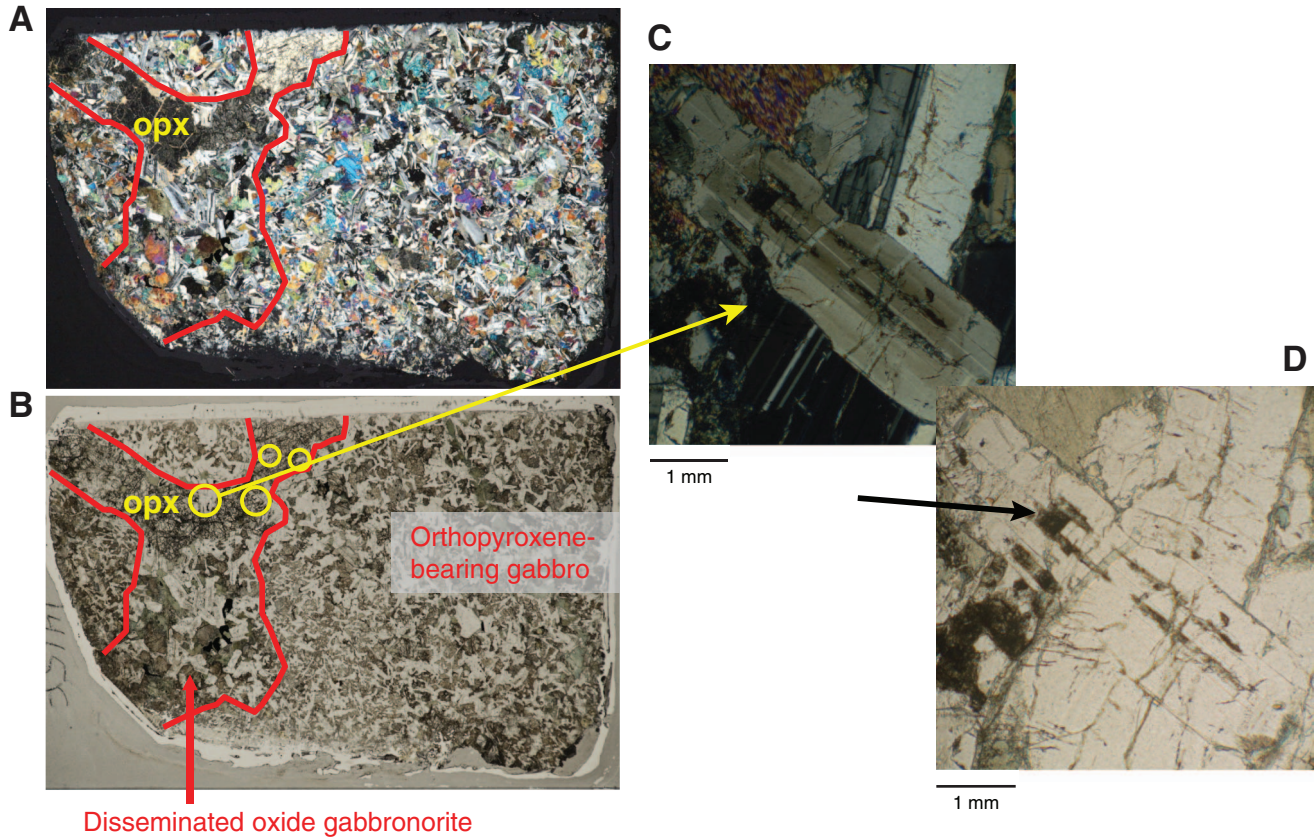


Figure F5. Highly altered troctolite (Sample 345-U1415E-1R-1, 30–33 cm [Piece 4]). The troctolite is equigranular rock with granular texture consisting of olivine (40%), plagioclase (45%), and clinopyroxene (15%), with trace amounts of oxide. Clinopyroxene occurs as subhedral to euhedral prismatic grains. Ol = olivine (completely altered to serpentine and magnetite), Pl = plagioclase, Cpx = clinopyroxene. **A.** Core close-up. **B.** Thin section image (Thin Section 2; plane-polarized light).

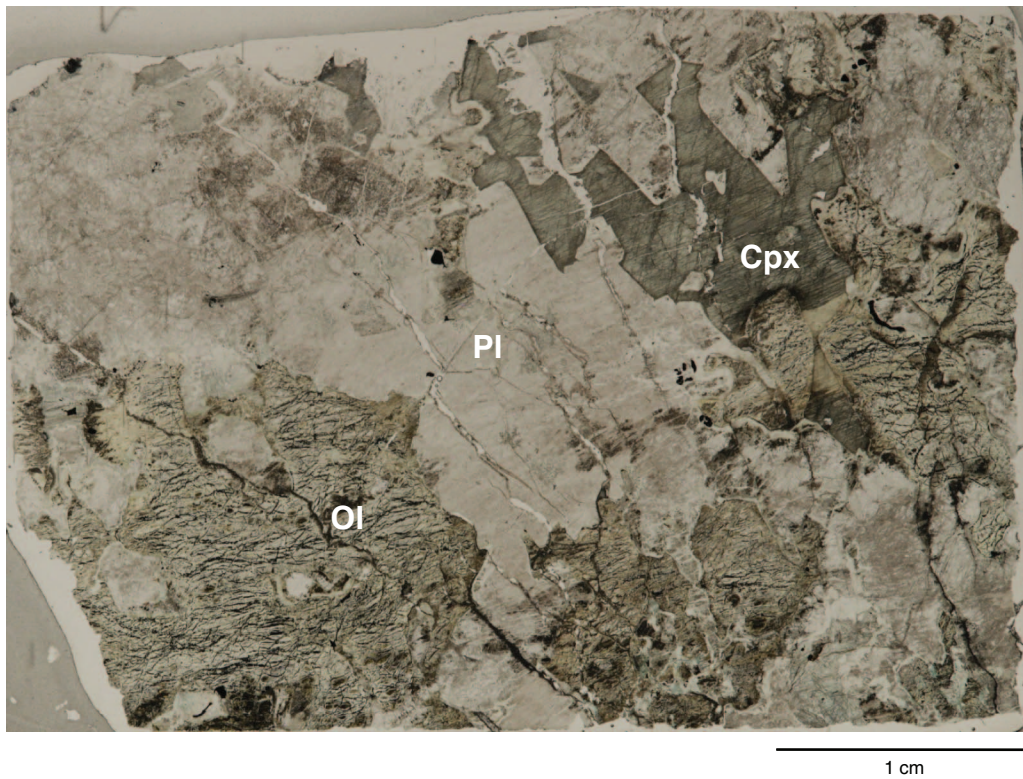
A**B**

Figure F6. Gabbronorite (Thin Section 1; Sample 345-U1415E-1R-1, 21–23 cm [Piece 3]). **A.** Patch (inferred to be an inclusion) of ophitic textured microgabbro (red outline) surrounded by coarser grained gabbronorite, in which pyroxene is pervasively replaced by green amphibole along fractures and cleavage planes. **B, C.** Detail from within the finer grained inclusion showing ophitic texture overprinted by grain boundary migration. Plg = plagioclase, Amph = amphibole, Cpx = clinopyroxene. **B** is under plane polarized light; **C** is under crossed polars.

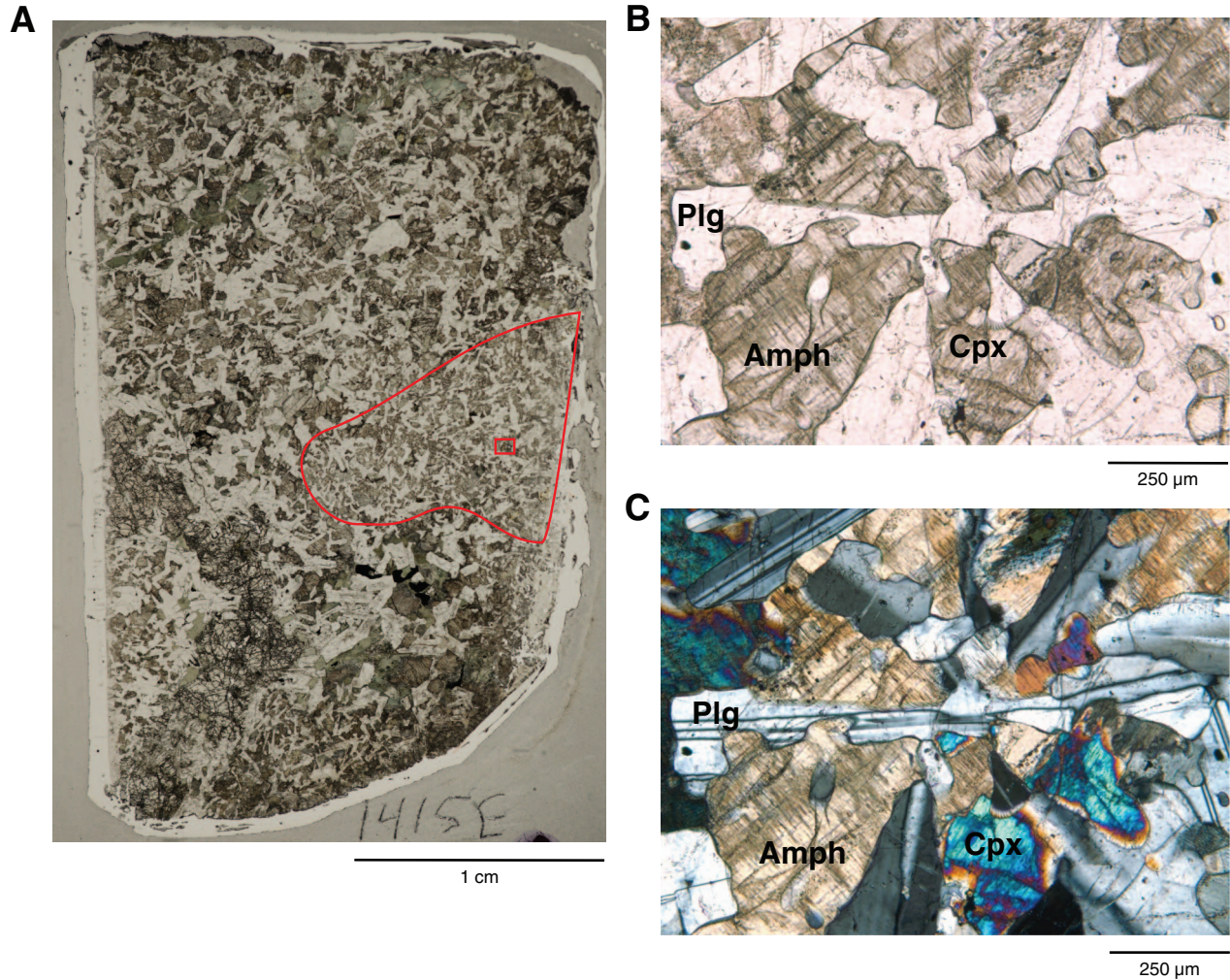


Figure F7. (A, B) Weak plagioclase shape-preferred orientation in gabbronorite (red arrow; Sample 345-U1415E-1R-1, 41–43 cm [Piece 5]) and (C) plagioclase crystals with large aspect ratios and seriate grain boundaries indicating grain boundary migration and recrystallization (gabbronorite; Sample 345-U1415E-1R-1, 21–23 cm [Piece 3]; under crossed polars). In A, red box (tick mark shows upward direction) indicates the location of the image shown in B. In B, detail shows multiple plagioclase crystals with deformation twinning, bending, and weak undulose extinction. The bending may result from elongate plagioclase crystals deforming around more rigid clinopyroxene crystals.

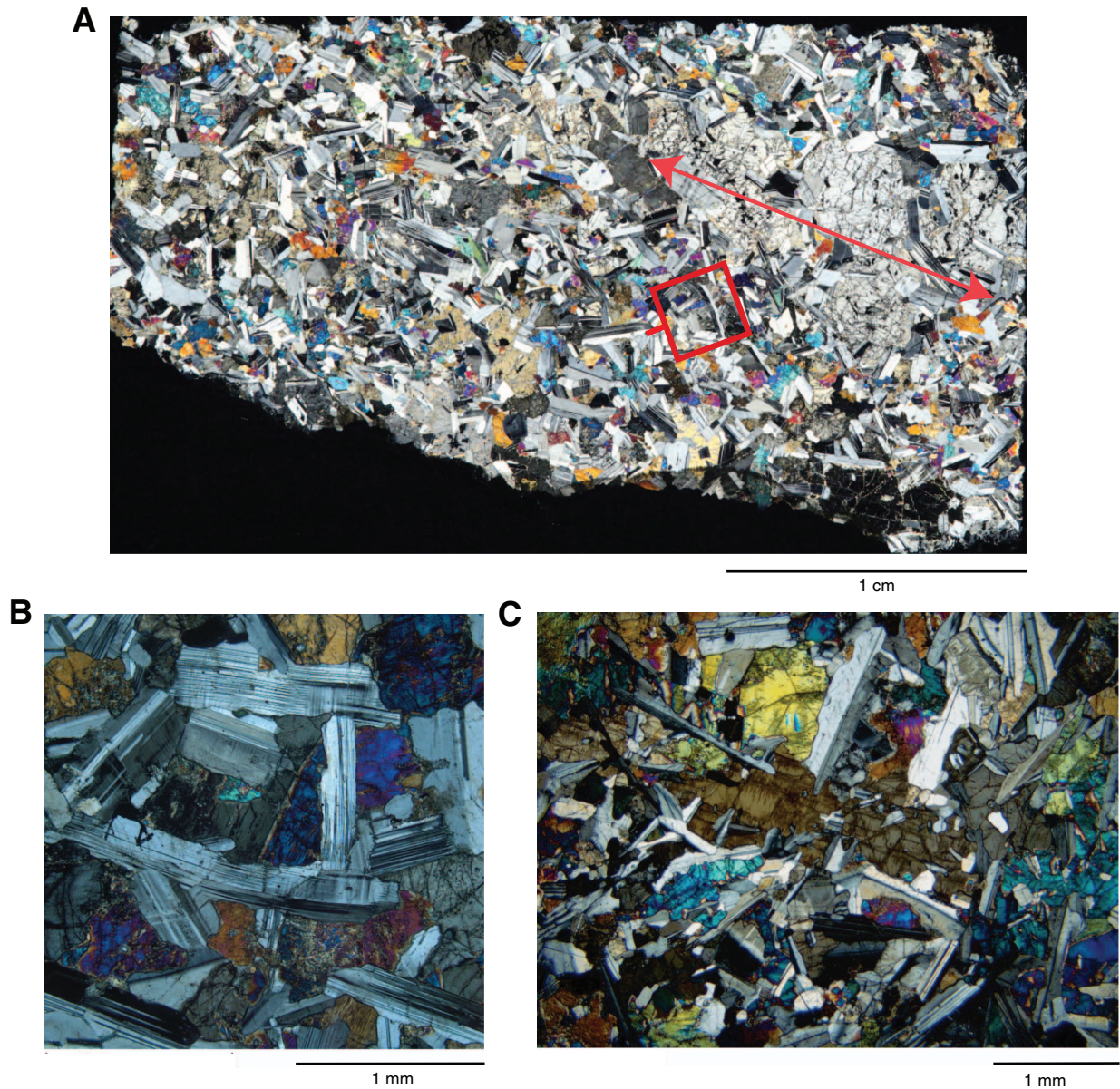


Figure F8. Vein contacts against host clinopyroxene-bearing troctolite showing no alteration halos (Sample 345-U1415E-1R-1, 30–33 cm [Piece 4]; under crossed polars). The section also shows crosscutting relationships with a prehnite vein cutting a serpentine vein.

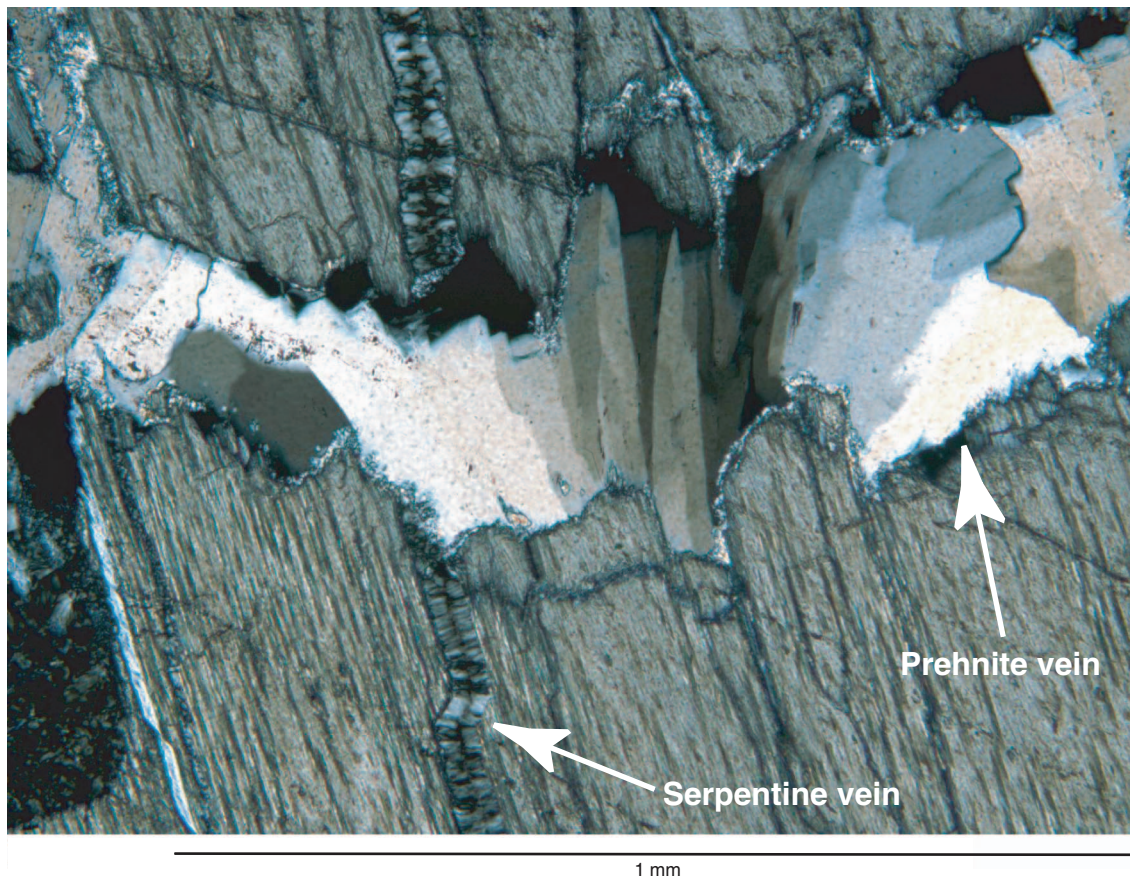


Table T1. Operations summary, Holes U1415D and U1415E.**Hole U1415D (jet-in test only; no coring):**

Latitude: 2°15.1437'N

Longitude: 101°32.7441'W

Time at site (h): 17.0 (0730 h, 24 December–0026 h, 25 December 2012)

Seafloor (drill pipe measurement below rig floor, m DRF): 4850.8

Distance between rig floor and sea level (m): 11.2

Water depth (drill pipe measurement from sea level, mbsl): 4839.6

Total penetration (drilling depth below seafloor, m DSF): 4.2

Hole U1415E (RCB coring):

Latitude: 2°15.1461'N

Longitude: 101° 32.7424'W

Time on site (h): 25.8 (0026 h, 25 December–0215 h, 26 December 2012)

Seafloor (drill pipe measurement below rig floor, m DRF): 4850.8

Distance between rig floor and sea level (m): 11.2

Water depth (drill pipe measurement from sea level, mbsl): 4839.6

Total penetration (drilling depth below seafloor, m DSF): 15.3

Total depth (drill pipe measurement from rig floor, m DRF): 4866.1

Total length of cored section (m): 15.3

Total core recovered (m): 0.84

Core recovery (%): 5

Drilled interval (m): 0

Total number of cores: 2 RCB

Core	Depth (mbsf)		Interval cored (m)	Core recovered (m)	Curated length (m)	Recovery (%)	Date (2012)	Time UTC (h)
	Top of cored interval	Bottom of cored interval						
345-U1415E-								
1R	0.0	10.3	10.3	0.54	0.62	5	24 Dec	1810
2R	10.3	15.3	5.0	0.30	0.31	6	24 Dec	2240
		Total:	15.3	0.84	0.93	5		

Local ship time was UTC – 7 h. DRF = drilling depth below rig floor, DSF = drilling depth below seafloor. R = rotary core barrel (RCB) system.



Table T2. Details and explanations for thin sections with two domains, Hole U1415E.

Core, section, interval (cm)	Thin section number	Lithologic interval	Rock name	Rock comment	Nature of domains	Contact	Number of domains	Igneous domain	Domain lithology name
345-U1415E-1R-1W, 21–23 (Piece 3)	1 (Image)	3	Orthopyroxene-bearing gabbro	With patches of coarser grained oxide-bearing gabbro	Two lithologies and textures	Sutured	2	1	Orthopyroxene-bearing gabbro
								2	Disseminated oxide gabbro